Title
EROSIVE WEAR OF DUCTILE METALS BY A PARTICLE-LADEN HIGH-VELOCITY LIQUID-JET

Author
Li, Simon Ka-Keung

Publication Date
1980-12-01

LBL-11959
Preprint

Lawrence Berkeley Laboratory
UNIVERSITY OF CALIFORNIA

Materials & Molecular Research Division

Submitted to Wear

EROSIVE WEAR OF DUCTILE METALS BY A PARTICLE-LADEN HIGH-VELOCITY LIQUID-JET

Simon Ka-Keung Li, Joseph A.C. Humphrey, and Alan Levy

December 1980

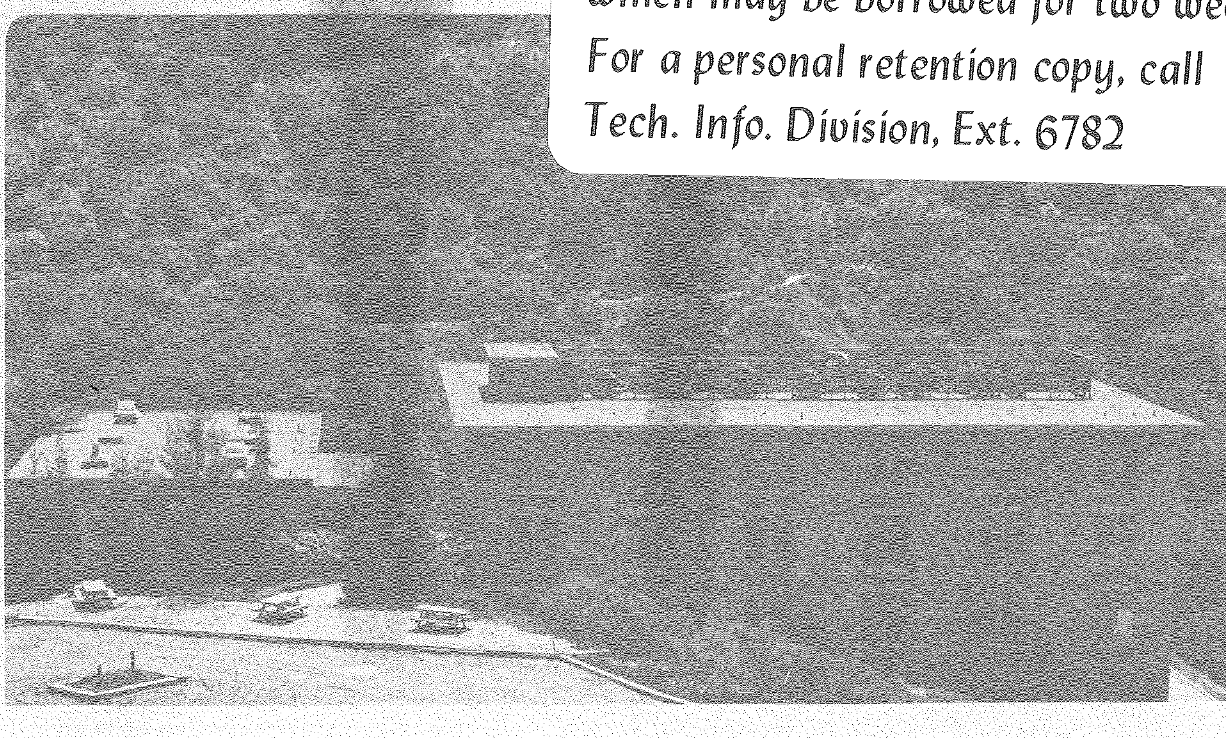

Prepared for the U.S. Department of Energy under Contract W-7405-ENG-48

LBL Report #11959

EROSIVE WEAR OF DUCTILE METALS BY A PARTICLE-LADEN HIGH-VELOCITY LIQUID-JET

by

Simon Ka-Keung Li

Joseph A.C. Humphrey

Alan Levy

December 1980

Materials and Molecular Research Division

Lawrence Berkeley Laboratory

University of California, Berkeley

Berkeley, CA. 94720

This work was supported by the Assistant Secretary for Fossil Energy, Office of Coal Research, Materials and Components Division of the U.S. Department of Energy under Contract Number W-7405-ENG-48 through the Fossil Energy Materials Programs, Oak Ridge National Laboratory, Oak Ridge, Tn.

ABSTRACT

A liquid-solid particle jet impingement flow apparatus is described and experimental measurements are reported for the accelerated erosion of copper, aluminum and mild steel sheet metal by coal suspensions in kerosene and alumina and silicon carbide suspensions in water. Slurry velocities of up to 130 ft/sec (40 m/sec) and impingement angles ranging from 15 degrees to 90 degrees were investigated. The maximum particle concentration used was 40% by weight. For high velocity the results of this study show two erosion maxima arising at impingement angles of 90 degrees and 40 degrees respectively, whereas in corresponding gas-solid particle investigations maximum erosion occurs at approximately 20 degrees. In the study both particle concentration and composition were varied. A polynomial regression technique was used to calculate empirical and semi-theoretical correlation constants.

NOMENCLATURE

C	Concentration (gr/cm^3)
dC_S/dt	Rate of erosive wear (gr/cm^2-sec)
D	Equivalent diameter (cm)
S	Yield stress or hardness ($dynes/cm^2$)
t	Time (sec)
V	Velocity (cm/sec)
δ	Characteristic viscous layer thickness (cm)
Δ	Weight loss per unit area (gr/cm^2)
μ	Viscosity (gr/cm^2-sec)
ρ	Mass density (gr/cm^3)

Superscripts

*	Denotes relative to liquid phase velocity

Subscripts

F	Refers to liquid phase
P	Refers to solid particle phase
S	Refers to eroded metal sample

CONTENTS

1. INTRODUCTION

The present energy shortage has brought to the attention of many researchers the need for alternative energy resources. Coal liquefaction is one of the most promising alternatives in the United States. Slurry transport is a primary consideration in coal liquefaction. The erosion by solid particles in a fluid stream has been a persistent problem in this process. The ability to predict the lifetime of flow components in a system is a major concern to both the operator and the designer. Unfortunately, there appear to be no reliable methods for the prediction of erosive wear under general conditions.

The rate of erosion cannot be determined easily due to the numerous and interrelated variables involved. The measurement of erosion rate can be made by several means, i.e., micrometers, profilometer, weight loss, ultrasonic thickness gages. All but the last method were used in this investigation.

Accelerated erosive wear provides a means of obtaining erosion data over short periods of time. Two devices have been used at this laboratory in earlier experiments, namely the slurry loop and the slurry pot [1]. Both devices have advantages and disadvantages. The slurry loop simulates an actual flow system in service and includes valves, pumps, piping, joints, elbows and contractions. While it accurately represents the effects of a slurry flow on component geometry it requires relatively long test times to obtain measureable data. Further difficulties arise in relation to measuring material losses periodically during a test and from the comminution of particles rounding off sharp edges which can lead to variations in fluid mechanic behavior during the course of an experiment.

The slurry pot does not measure wear on flow components, but it provides a measure of wear of cylindrical metal samples in a relatively short time. It presents the distinct advantage of allowing quick and easy changes in experimental conditions. Another important feature of the slurry pot is that it can be appropriately modified to operate at the higher temperatures characteristic of coal liquefaction processes. The primary shortcomings of this tester are the unknown fluid mechanic characteristics of the flow and the uncontrolled occurrence of particle comminution.

The Jet Impingement Tester (JIT) was developed to account for some of the limitations of the slurry loop and slurry pot. Because it utilizes the particles in the slurry once only it can be used to study the effect of impingement on a flat metal surface without being complicated by the factor of comminution (particle breakdown). The JIT can be used conveniently to study the effect of impingement angle on erosion, a factor of considerable importance. In the present study, SiC and Al_2O_3 particles were used in addition to coal to eliminate the uncertainty associated with the complicated composition and structure of coal when determining the effects of slurry variables on the erosion of metals. Water was used as the carrier fluid in addition to kerosene in order to simplify the problem of waste disposal of the slurries and to provide a liquid with a viscosity different from that of kerosene.

2. EXPERIMENT

2.1 Description of Experimental System

The experimental system is shown in Fig. 1-a. It consists of an 80 gallon holding tank, compressed nitrogen gas bottles, an electric mixer, sections of pipe-line, a metal sample holder, a sample holder compartment and a waste tank for the used slurry. The compressed gas is used to drive the slurry through a 1/8" diameter nozzle, 1/2" in length, that is located inside the sample holder compartment. See figure 1-b for a detailed drawing. Different flow velocities can be obtained by setting the regulator to different pressures. The propeller type electric mixer is used to keep the particles in complete suspension during the course of an experimental run. The sample holder is capable of being adjusted to any desired angle between 0 and 90 degrees and accepts specimens 3/4 × 1 1/4 inches and up to 1/8 inch thick. The tank and the pipe line imposed no practical limitations on the particle concentration of the slurry. Concentrations of up to 40% by weight were used.

2.2 Experimental Methodology

Because of the many variables governing the erosion of metals, the experimental determination of the effects of all their possible combinations on erosive wear is not practically feasible. Careful consideration has been given to determining the most important variables which can be divided into three groups: (a) fluid properties, (b) target material properties and (c) particle properties. A list of eleven variables considered to be of importance to this study has already been given in [1,2]. In addition, orientation angle must now be considered. From these, nine non-dimensional groups my be formed. A detailed consideration of these groups along the lines of [1] reduces to five the number of dimensionless parameters required to characterize the present flow. Even with only five non-dimensional parameters, the number of data points needed to derive an accurate empirical correlation is still large. In an effort to reduce the number of experiments, when investigating the influence of one parameter the remaining parameters were held constant at intermediate values of their possible ranges. In this way, the relative influence of all the variables was dealt with and the relative importance of each was determined.

2.3 Procedure

Briefly, the operating procedure for an experimental run was as follows. The appropriate amount of sieved particulate material was weighed out to make solutions of 10%, 20%, 30% and 40% by weight respectively. The holding tank was filled with the required amount of liquid, the mixer was turned on and the particles added to the liquid. Approximately 15 gal. of slurry were used for each test. A polished metal specimen was firmly placed in a sample holder at the proper orientation angle. The test was initiated by turning an on-off valve above the nozzle, with stop-watch timing to determine the amount of slurry used, based upon careful pre-calibration of the system. Pressure in the nitrogen bottles was regulated to obtain the desired slurry velocity. The valve was turned off after the required amount of slurry impacted the specimen.

3. RESULTS AND DISCUSSION

Three different flat metal samples, OFHC copper, 6061-T6 aluminum alloy and 1018 mild steel were investigated. Table 1 gives the properties of the materials used.

Measurements of erosive wear in units of test sample weight loss per unit weight of erosive particles are plotted as a function of velocity for a 20 wt% coal-kerosene slurry in Fig. 2. Similar results for various combinations of Al_2O_3 and SiC slurries are shown in Fig. 3. All of the data for the different test conditions indicate that erosive wear varies approximately with the square of jet velocity (see Table 2). The square power dependence on velocity confirms the important role played by the kinetic energy of the impacting particles in the erosion process. Further consideration of the data in Figure 3 shows that pure SiC particle suspensions eroded more metal sample material per unit weight than did the pure Al_2O_3 suspensions. In addition, although there is scatter in the data it appears clear that of the two mixtures, that with 75% SiC was the more erosive of the two. In fact, differences between the 100% and 75% SiC curves are within the uncertainty of the measurements and, it must be concluded, are not significant. The large difference arising between the 100% and 75% Al_2O_3 curves is due mainly to the difference in concentration between these two runs.

Figures 4 and 5 show the effect of erosion on the three target materials. Fig. 4 shows that the erosion in coal-kerosene slurries generally decreased with increased metal hardness but not in a direct proportion to the hardness difference [3]. Fig. 5 shows a similar variation of erosion with metal hardness for the Al_2O_3, SiC water slurries. The figure also supports the general observation that variations in slurry particle composition affected erosion only weakly. Nevertheless, erosion by the Al_2O_3 and SiC slurries was approximately two orders of magnitude larger than by a coal slurry for similar conditions.

Figures 6-9 show the effect of jet impingement angle on erosive wear. Fig. 6 shows the appearance of the eroded surface as a function of angle. The ripples that form at shallow impingement angles in the gas-solid particle erosion of ductile metals are seen to occur at steep as well as at shallow angles in the liquid-solid particle erosion. The hills and valleys (moguls) that occur at steep angles in gas-solid particle erosion were not observed. This result, and the shape of the curves in Fig. 7-9 suggest that a different erosion mechanism may be taking place in the present liquid-solid particle erosion investigation and in liquid-solid particle erosion systems in general.

Fig. 7 shows plots of erosion vs. impingement angle for 6061-T6 aluminum alloy in a 20 wt% coal-kerosene slurry. It can be seen that the erosion increases with angle, peaking at 90°. For comparison, the dotted curve is a typical plot of aluminum eroded by a gas-solid particle flow taken from [4]. Although erosive wear values for the two curves differ by three order of magnitude, the difference in the shape of the two curves suggests yet again that the erosion mechanisms for the two media may be significantly different. The shape of the coal-kerosene curve is very similar to that which occurs for brittle materials in gas-solid particle erosion. The reasons for these differences must be determined in future work.

Fig. 8 for the Al_2O_3, SiC-water slurry erosion tests at low velocities (50-60 ft/sec) also shows maximum erosion occuring at a jet impingement angle of 90 degrees for all of the particle mixtures tested. The increase in erosion arising with increasing hardness and/or integrity of the particles going from Al_2O_3 to SiC also differs from the behavior observed in gas-solid particle erosion where essentially no difference in erosion occurs between the two types of particles.

Fig. 9 shows similar plots of erosion vs. impingement angle for higher velocities (70-74 ft/sec). Yet another phenomenon differing significantly from gas-solid particle erosion is observed. A minimum in erosion appears at an angle of approximately 60 degrees suggesting a transition between two possible erosive wear mechanisms associated with the respective peaks at 90 and approximately 40 degrees. A metallographic analysis of specimens exposed to the two erosion regimes may help clarify the nature of the wear mechanisms involved.

Figures 10 and 11 indicate the effect of particle concentration on erosion. Fig. 10 shows that for coal in kerosene, erosion increases with an increase in particle concentration. The flattening of the curve at 30 wt% suggests only a weak dependence of erosion on particle concentration for typical coal liquefaction systems (30-50 wt% coal). Fig. 11 shows that for Al_2O_3 in water, erosion increases with an increase in particle concentration between 10 and 20 wt% but decreases with an increase in particle concentration between 20 and 30 wt%.

4. CORRELATION OF THE RESULTS

The complex dependence of erosion on jet impingement angle precludes finding a simple mathematical function describing the relative influence of this parameter. Because of this the correlations presented below were derived for 90 degree impingement angle data only, for which maximum erosion occurs. The form of the empirical correlation used was:

$$\frac{dC_S/dt}{V_P C_P} = f\left[\frac{D_P \rho_F V_P^*}{\mu_F}, \frac{\delta}{D_P}, \frac{\rho_P}{\rho_F}, \frac{V_P^*}{V_P}, \frac{C_P}{\rho_P}, \frac{S_S}{\rho_P V_P^2}, \frac{S_P}{S_S}\right] \tag{1}$$

The derivation of equation (1) will be found in reference [1] where it is shown how, for conditions similar to those of the present study, it reduces to:

$$\frac{dC_S/dt}{V_P C_P} = A \left(\frac{\rho_P}{\rho_F}\right)^a \left(\frac{C_P}{\rho_P}\right)^b \left(\frac{S_S}{\rho_P V_P^2}\right)^c \left(\frac{S_P}{S_S}\right)^d \tag{2}$$

The term on the left hand side of equation (2) has the same physical meaning and can be shown to correspond exactly to the dimensionless erosive wear parameter shown on the figures. A semi-theoretical correlation suggested by Humphrey [2] and given by equation (3) below was also used in the correlation study.

$$\frac{dC_S/dt}{V_P C_P} = A \left(\frac{\rho_P}{\rho_F}\right)^a \left(\frac{C_P}{\rho_P}\right)^b e^{-c\, S_S/\rho_P V_P^2}\, e^{d\, S_P/S_S} \tag{3}$$

Table 3 lists those constants providing the best regression curves for the experimental data which are consistent with physical reality over the experimental ranges for which they were derived. It will be noticed that the parameter S_P/S_S is excluded in the final correlations. In fact, fits with this term included yielded slightly less accurate and/or physically unrealistic functional forms for erosion than did fits without the term. The reason for this is attributed to the relatively small difference in hardness between Al_2O_3 and SiC particles (see Table 1) which the correlations cannot detect within the uncertainty of the measurements. A larger body of experimental data would be required to compute a trust-worthy exponent for the parameter S_p/S_S. Thus, the correlations provided are recommended for systems with particles in suspension of similar hardness to those used in the present study.

Inspection of the empirical regression coefficients indicates a quadratic dependence of wear on velocity as was previously noted. A cubic dependence on particle concentration also demonstrates the relatively large importance of this effect. For the conditions of the JIT experiment the rate of wear is seen to be inversely proportional to particle density. This contrasts sharply with the slurry pot study results [1] where a direct proportionality was found. It must be concluded that the fluid mechanic characteristics peculiar to each system play leading roles in determing the manner and rate by which the wear processes occur and hence the form of the correlations.

5. ERROR ANALYSIS

Many factors affect the precision of the experimental results. However, due to the nature and complexity of the experiment and the number of the variables involved, none of the experiments was performed more than once. Hence, the standard procedure of taking the standard deviation of several replicate measurements was not possible. Nevertheless, an error analysis was performed.

Rearranging the empirical correlation with only the terms $\frac{P}{F}$, $\frac{C_P}{P}$, $\frac{S_S}{\rho V_P^2}$ considered, yields:

$$\frac{dC_S/dt}{V_P C_P} = A' \; C_P^{\,b} \; V_P^{\,-2C} \tag{4}$$

In the above equation A' contains all terms which did not contribute significantly to the error. Thus, the major sources of error arose from the measurements of C_P and V_P with the latter approximated as the jet velocity. From equation (4) it is readily shown that

$$e\left[\frac{dC_S/dt}{V_P C_P}\right] = b \; e \; [C_P] - 2c \; e[V] \tag{5}$$

where e denotes relative error of the bracketed term.

Estimates of $e[C_P]$ and $e[V_P]$ derived from the experimental conditions were ± 0.017 and ± 0.060 respectively. Substitution of these values into equation (5) together with values of the exponents from Table 3 yielded $e\left[\frac{dC_S/dt}{V_P C_P}\right] = \pm\, 5.0\%$ approximately. This relative error denotes the worst possible case and is of the order of the scatter in the data.

Average relative errors arising between measured and calculated erosive wear, using equations (2) and (3), are indicated in Figure 12 for different slurries. The figure provides a relative comparison of the two calculation approaches. The total number of data points used for the fits was 22. It is seen that the total average errors derived from the fits are in reasonable agreement with the error analysis result.

6. CONCLUSIONS

1. It has been demonstrated that a liquid jet impingement tester generates useful reproducible erosive wear data over a wide range of testing conditions in a relatively small amount of time and reasonably accurately.
2. The erosion rate of both mild steel and 6061-T6 aluminum alloy in a coal-kerosene slurry had a velocity exponent of 2, strongly supporting the notion that the kinetic energy of the particles relates directly to the erosion process. Erosion of the aluminum alloy in the Al_2O_3, SiC-water slurries showed a similar dependence on particle velocity.
3. The erosion rate of the alloys in Al_2O_3, SiC-water slurries was two orders of magnitude higher than that in the coal-kerosene slurries.
4. Erosion of copper, aluminum and steel varied directly with the hardness of the target metal.
5. A rippled pattern occurred on the erosion surface of specimens tested at <u>all</u> impingement angles up to 90 degrees. The absence of the mogul pattern (hills and valleys) which occurs in gas-solid particle erosion at steep angles of jet incidence strongly suggest that a different erosion mechanism may be involved in liquid-solid erosion processes.
6. The erosion rate of 6061-T6 aluminum alloy increased with impingement angle to a maximum at 90 degrees. This behavior is markedly different from ductile metal erosion in gas-solid particle flow where the erosion rate peaks at an impingement angle of about 20 degrees, further indicating that the erosion mechanism is probably different.

7. The erosion rate of aluminum alloy by Al_2O_3, SiC-water slurries also peaks at a 90 degrees impingement angle, but shows a minimum in the rate-angle curve at about 60 degrees which is not observed in gas-solid particle erosion.
8. The erosion rate of 6061-T6 aluminum increases with coal concentration until about 30 wt% at which point the curve flattens out. This suggests that for typical coal liquefaction system concentrations (30-50 wt%) further increases in particle concentration will not significantly increase erosion.
9. The total average absolute value of the predictive error of the empirical fit was found to be 5.84% while that for the semi-theoretical fits was 6.72%. The present erosive wear correlations differ significantly from those obtained earlier in a slurry-pot tester. This suggests that the specific fluid mechanic features of an erosion process are very important in determining the nature and rate of wear of ductile metals.

ACKNOWLEDGEMENTS

The authors wish to express their sincere appreciation to D. Boone and T. Britt for their interest and helpful assistance in the course of this work. The bulk of this report is based on an M.Sc. thesis research project conducted by the first author in the Mechanical Engineering Department, University of California at Berkeley.

This work was supported by the Assistant Secretary for Fossil Energy, Office of Coal Research, Materials and Components Division of the U. S. Department of Energy under Contract Number W-7405-ENG-48 through the Fossil Energy Materials Programs, Oak Ridge National Laboratory, Oak Ridge, TN.

REFERENCES

1. W. Tsai, J.A.C. Humphrey, I. Cornet and A. Levy, "Experimental Study of Erosive Wear in a Slurry Pot Tester", presented at the ASME Winter Annual Meeting, Polyphase Flow Transport Conference, San Francisco, August 1980. To appear in WEAR 1981.

2. J.A.C. Humphrey, "A Transition State Model for Predicting the Rate of Erosive Wear of Ductile Material by Solid Particles". To appear in WEAR 1981.

3. J.E. Goodwin, W. Sage and G.P. Tilly, "Study of Erosion by Solid Particles", Proc. Inst. of Mech. Engrs., 184, pp. 279-292, (1969).

4. I. Finnie, A. Levy, and D.H. McFadden, "Fundamental Mechanisms in the Erosive Wear of Ductile Metals by Solid Particles", ASTM STP 664 Erosion Prevention and Useful Applications, pp. 36-58, (1979).

5. R.C. Weast, ed., Handbook of Chemistry and Physics, 51 edition. The Chemical Rubber Company, Cleveland, Ohio, 1970.

6. ASM Metal Handbook Vol. 1, Properties and Selection of Metals, 8th edition.

7. Metal Progress Data Book 1978. Mid June.

8. V.L. Streeter, ed., "Handbook of Fluid Dynamics", McGraw-Hill, New York, 1963.

TABLE 1: Estimated Properties

Particles (reference 5)

	Density (g/cm^3)	Average Hardness (Mohs scale)	Equivalent Diameter (μm)
Coal	1.5	2.21	24
Al_2O_3	4.02	9.0	150
SiC	3.22	9.5	150

Metals (references 6 and 7)

	Average Hardness (Brinell scale)	Average Yield Stress ($dynes/cm^2$)
OFHC Copper	44	$2.48\ 10^9$
6061-T6 aluminum	95	$2.75\ 10^9$
1018 mild steel	133	$3.44\ 10^9$

Solvent (reference 8)

	Density	Viscosity
Kerosene	$0.816\ g/cm^3$	$1.819\ 10^{-2}$ g/sec-cm
Water	$1.000\ g/cm^3$	$1.006\ 10^{-3}$ g/sec-cm

TABLE 2: Empirical correlation between erosive wear and jet velocity. Due to the no-slip assumption suspended particles are presumed to be moving at the velocity of the liquid jet.

Mixture used	Correlation
100% Al_2O_3	Erosion = $7.77 \times 10^{-10} V^{1.94}$
100% SiC	Erosion = $3.87 \times 10^{-10} V^{2.19}$
20% mixture 25/75 Al_2O_3/SiC	Erosion = $7.22 \times 10^{-10} V^{2.04}$
20% mixture 25/75 SiC/Al_2O_3	Erosion = $8.04 \times 10^{-10} V^{2.00}$
100% coal	Erosion = $2.49 \times 10^{-11} V^{1.98}$

TABLE 3: Fitted Coefficients and Parameter Ranges for Equations (2) and (3)

Coefficient	Empirical Fit	Semi-Theoretical Fit
A	0.33×10^{-5}	0.12×10^{-6}
a	1.10	- 0.12
b	2.20	1.09
c	- 0.51	0.16×10^{-6}
d	0	0

Parameter Ranges

$$0.895 \times 10^{-8} < \frac{\frac{dC_S}{dt}}{V_P C_P} < 0.27 \times 10^{-7}$$

$$3.218 < \frac{\rho_P}{\rho_F} < 4.022$$

$$0.266 < \frac{C_P}{\rho_P} < 3.605$$

$$592.75 < \frac{S_S}{\rho_P V_P^2} < 7416.92$$

and

$$\frac{\delta}{D_P} \leqslant 1 \ , \ \frac{D_P \ \rho_F V_P^*}{\mu_F} \simeq 0 \ , \ \frac{V_P^*}{V_P} \simeq 0$$

FIGURE CAPTIONS AND FIGURES

1a. Schematic diagram of the Jet Impingement Tester.

1b. Detailed drawing of jet nozzle.

2. Effect of velocity on erosion of aluminum and 1018 mild steel by coal slurry.

3. Effect of velocity and concentration on erosion of aluminum and copper samples by Al_2O_3, SiC slurries.

4. Effect of material variation on erosion by coal slurry.

5. Effect of material variation on erosion by Al_2O_3, SiC slurries.

6. Photographs showing samples at different angles after being eroded by 20% Al_2O_3 at 70 ft/sec.

7. Effect of angle on erosion by coal slurry.

8. Effect of angle and composition on erosion by Al_2O_3, SiC slurries at low velocity.

9. Effect of angle and composition on erosion by Al_2O_3, SiC slurries at high velocity.

10. Effect of particle concentration on erosion by coal slurry.

11. Effect of particle concentration on erosion by Al_2O_3 slurry.

12. Relative comparison of predicted and measured erosive wear: o empirical fit: o semi-theoretical fit. Data corresponds to α = 90 degrees, and the use of equations (2) and (3) with constants taken from Table 5.

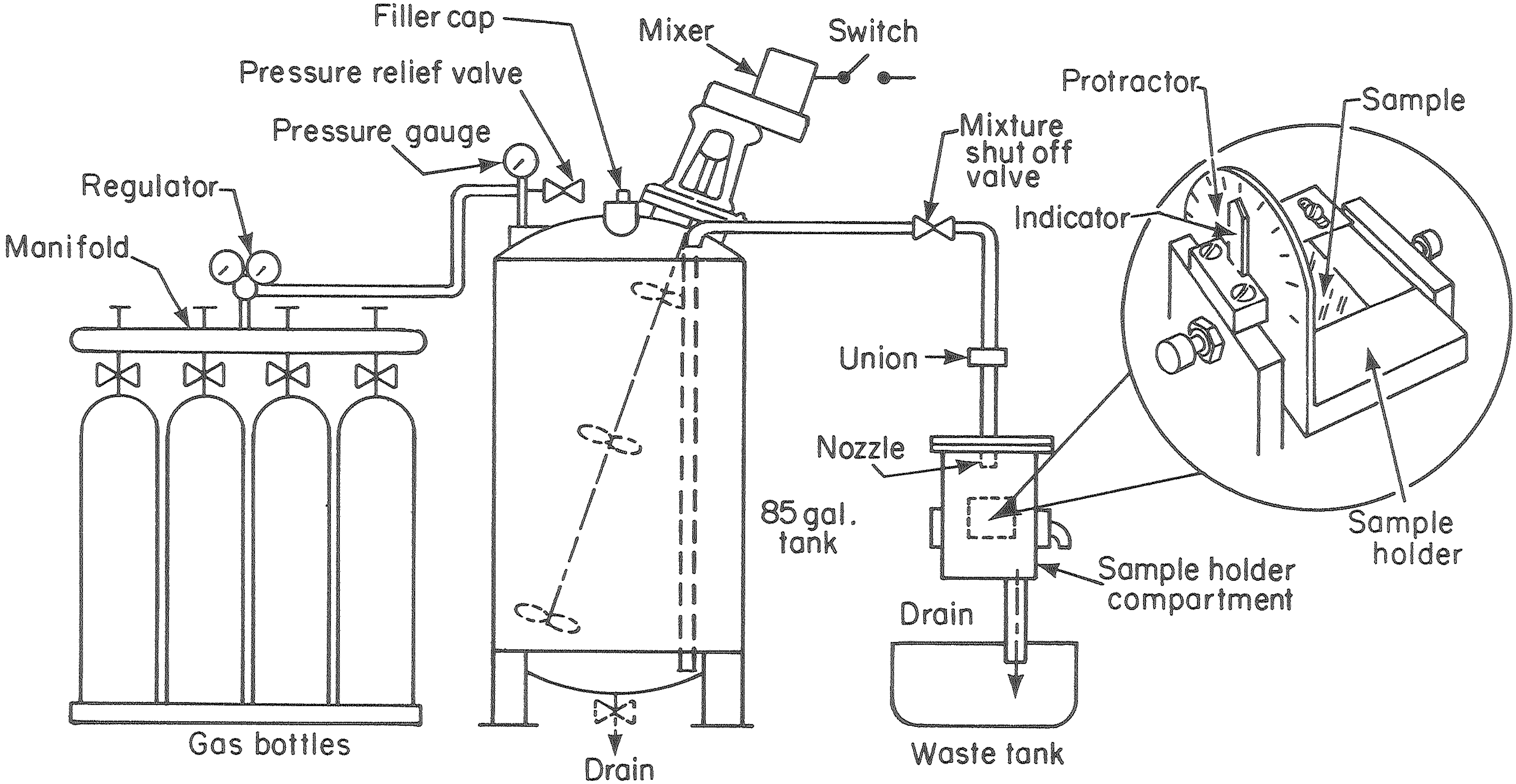

Fig. 1a

XBL 816-932

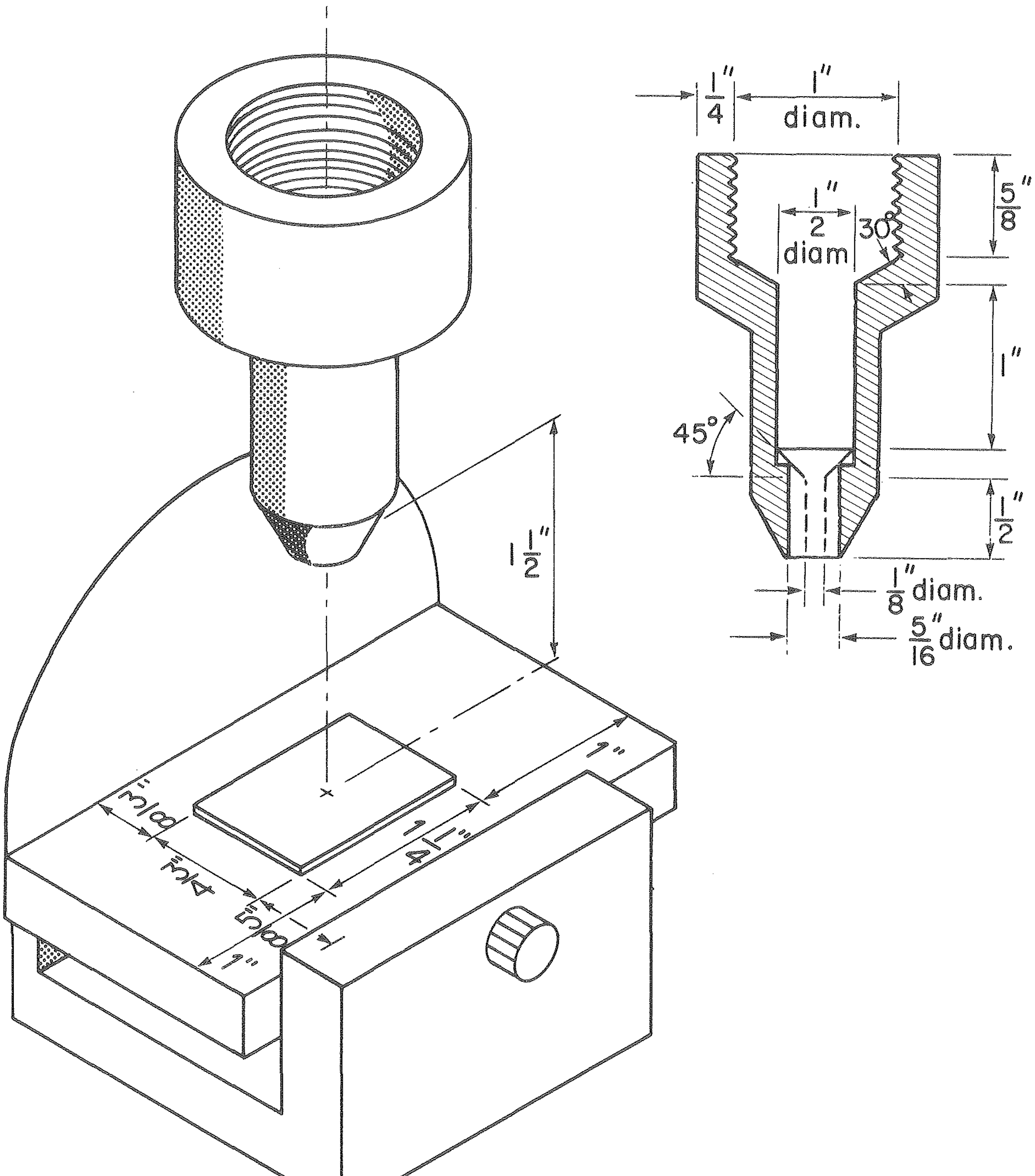

Fig. 1b

XBL816-933

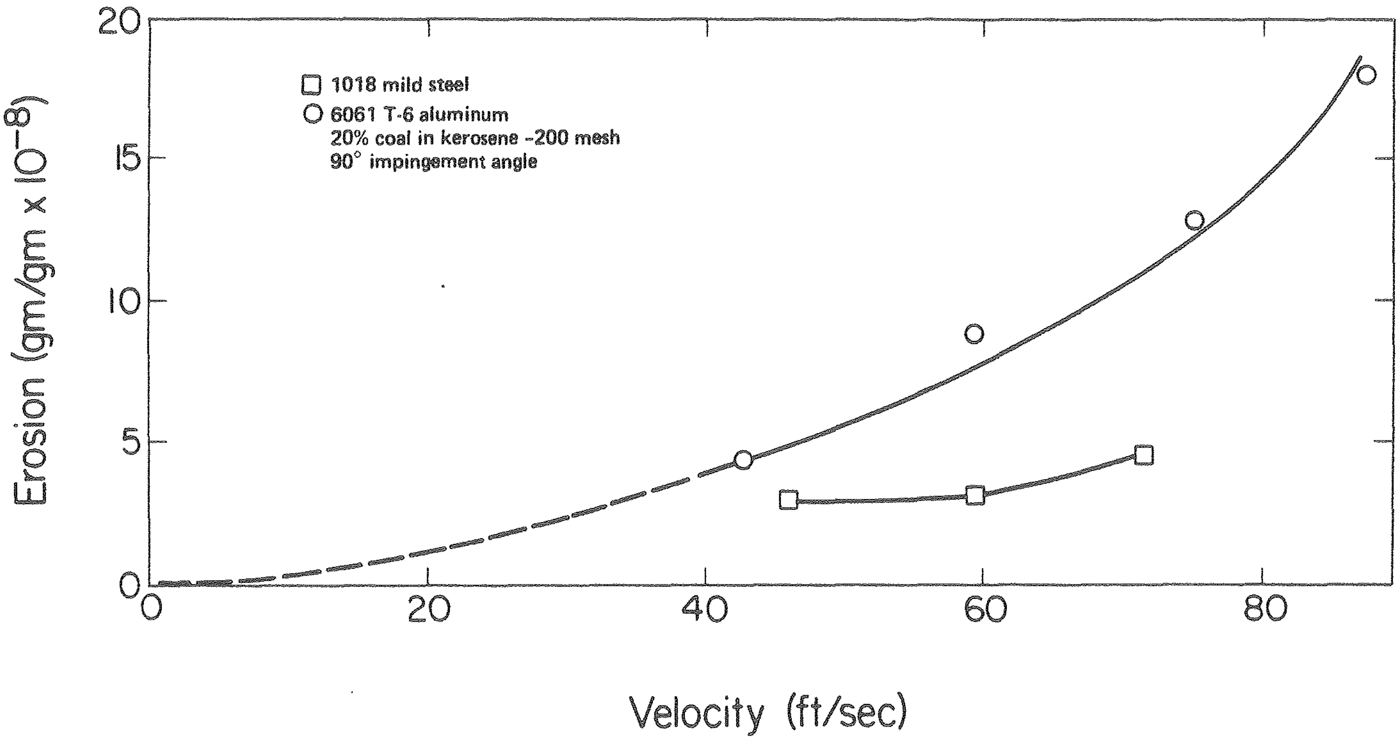

Fig. 2

XBL 8012-2450

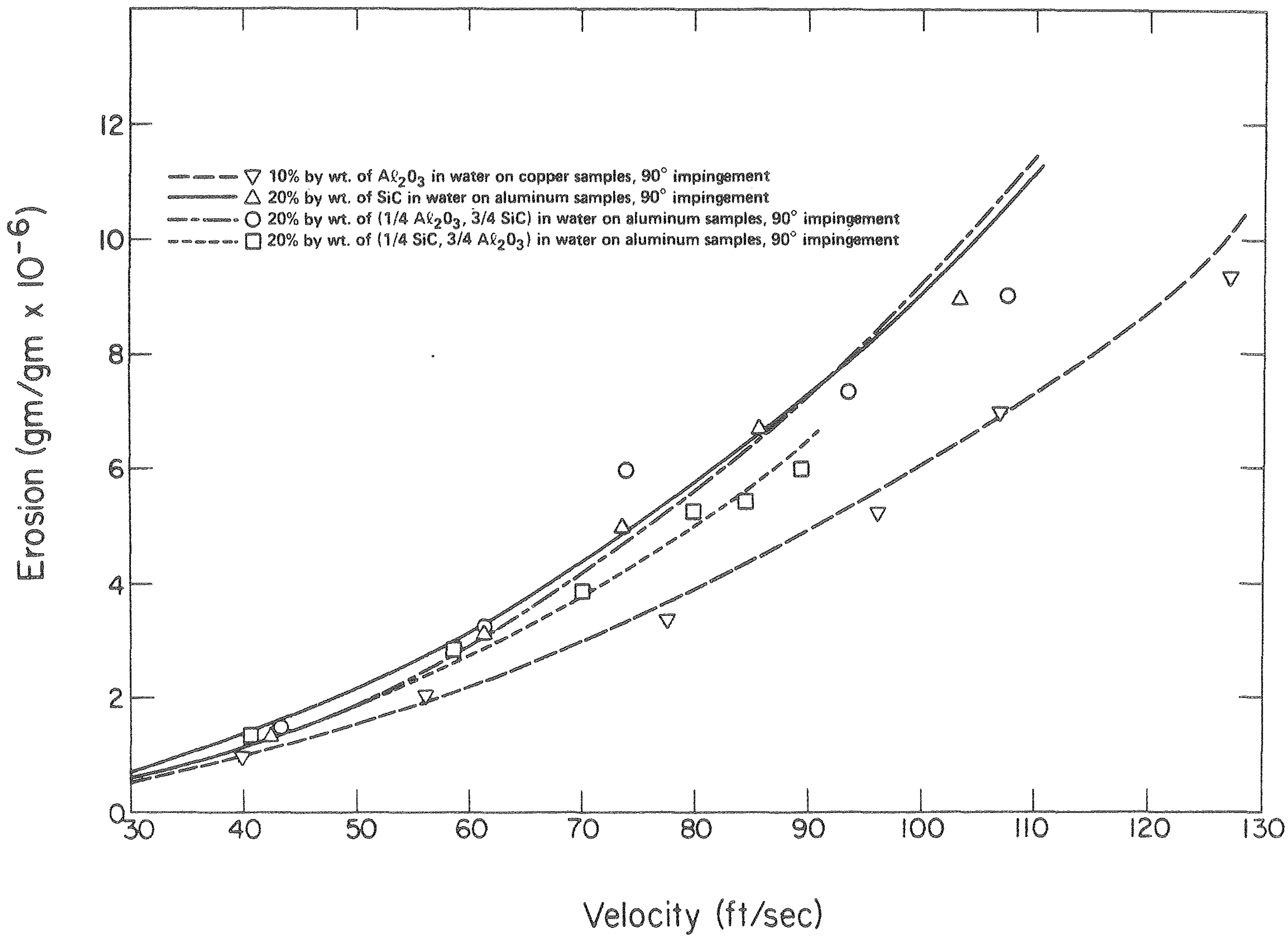

Fig. 3

XBL 8012-2453

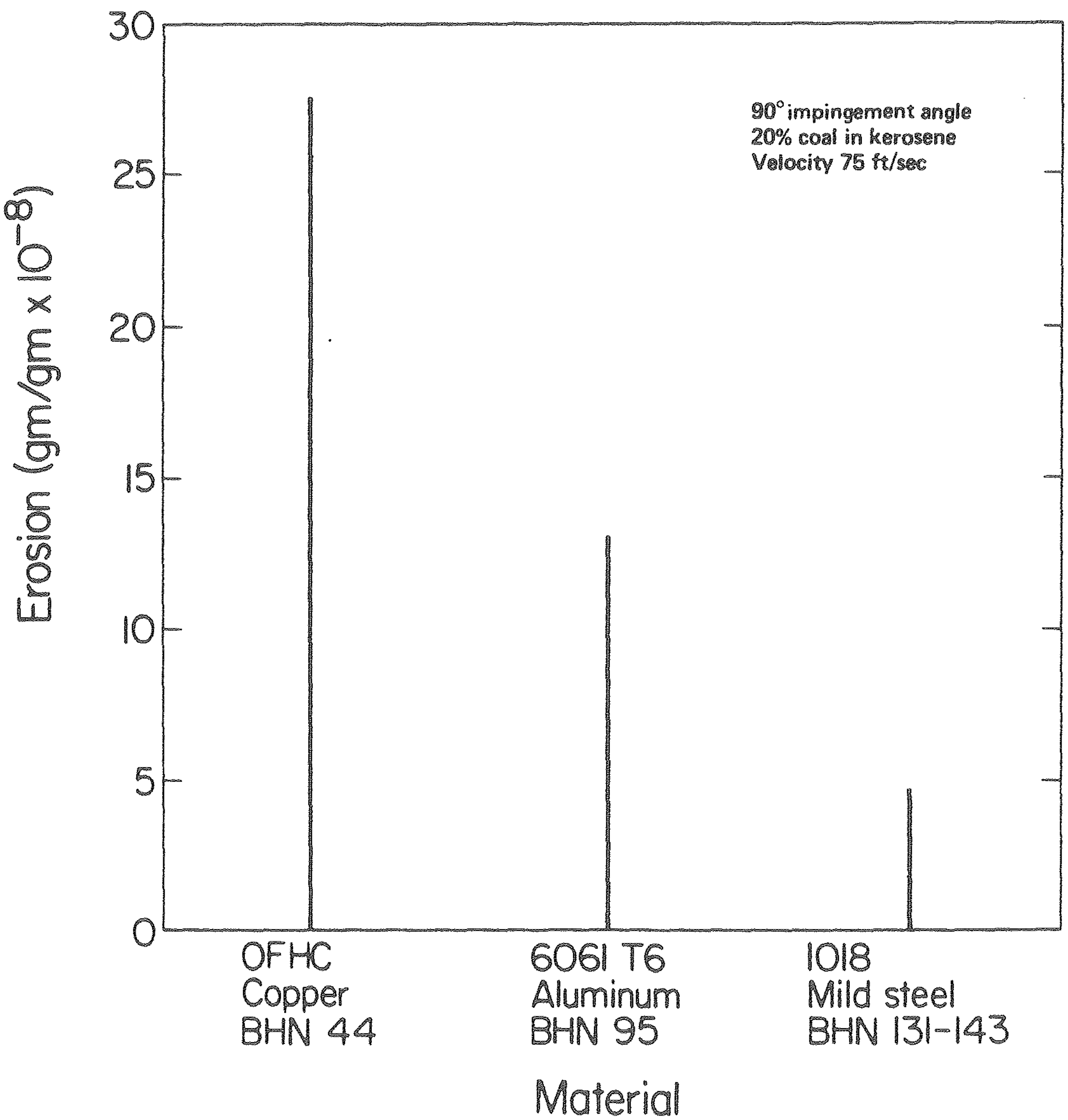

Fig. 4

XBL 8012-2449

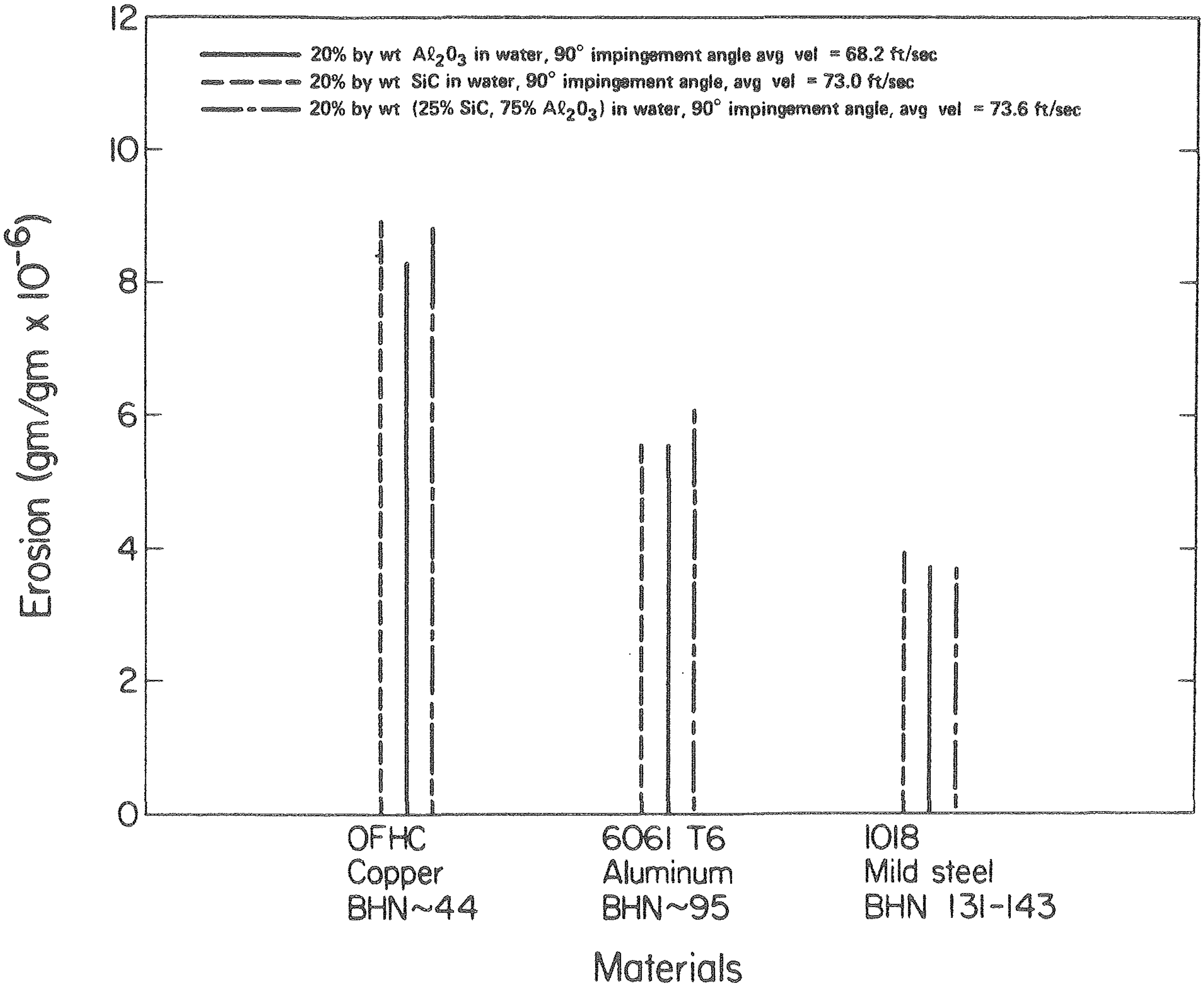

Fig. 5

XBL8012-2454

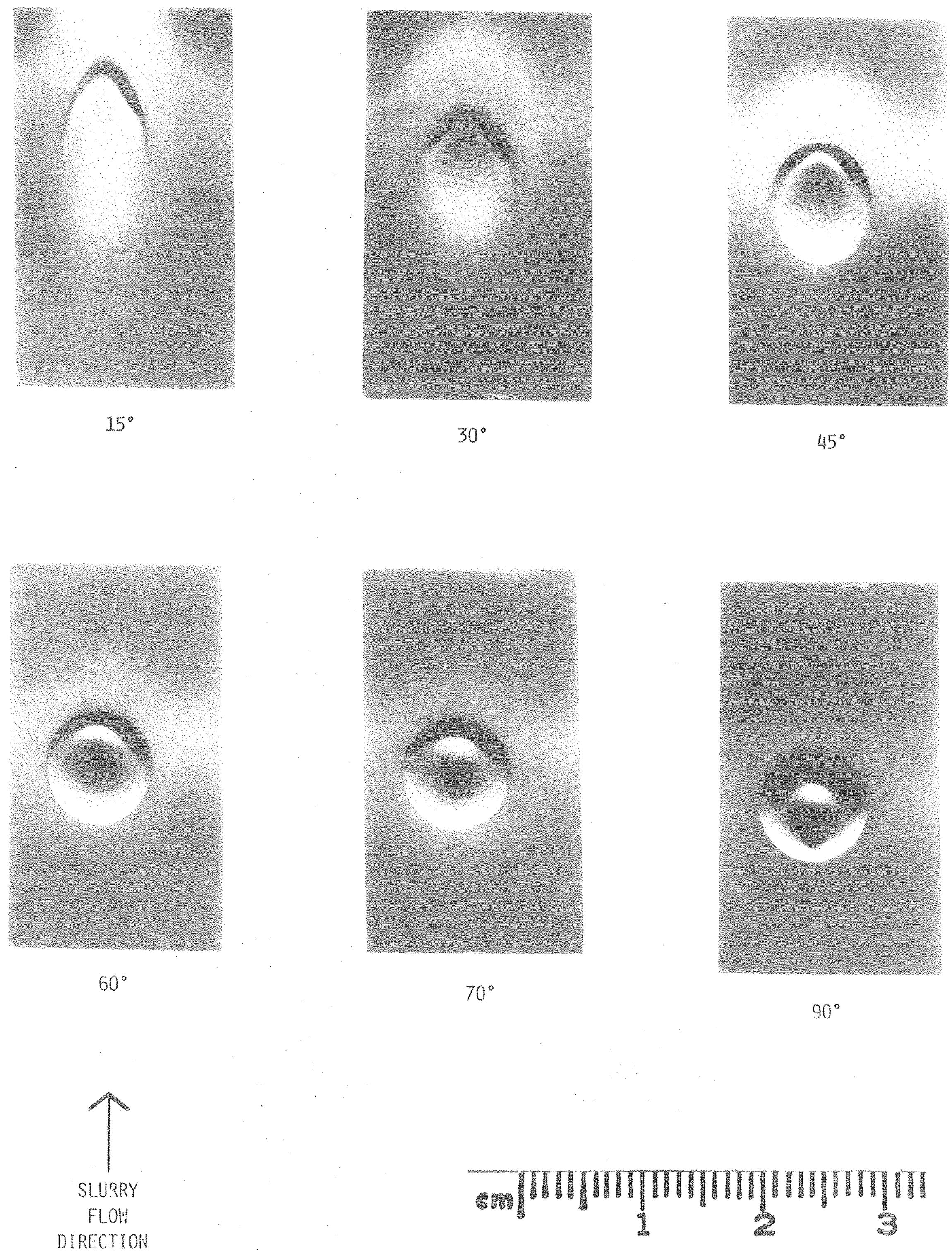

Fig. 6

XBB 815-4078

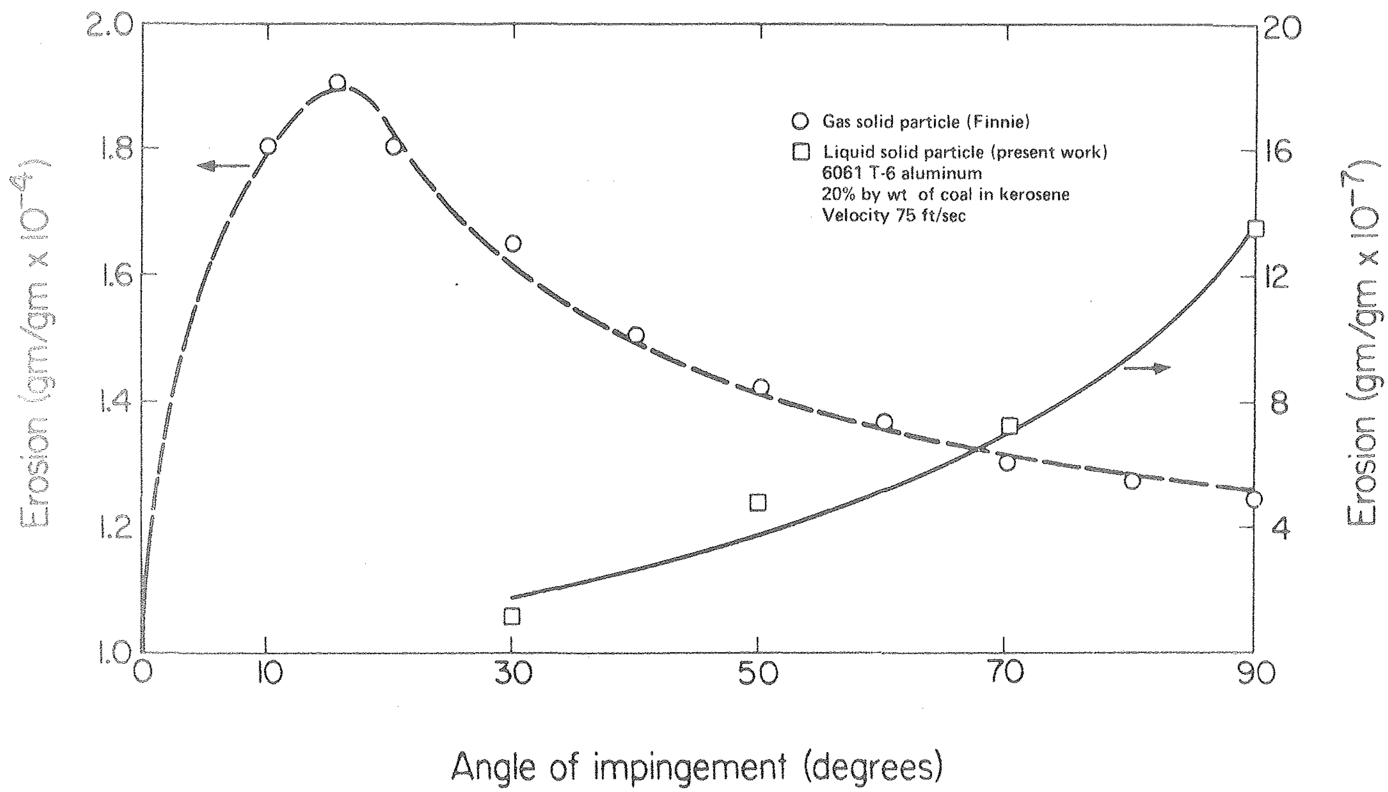

Fig. 7

XBL 8012-2451

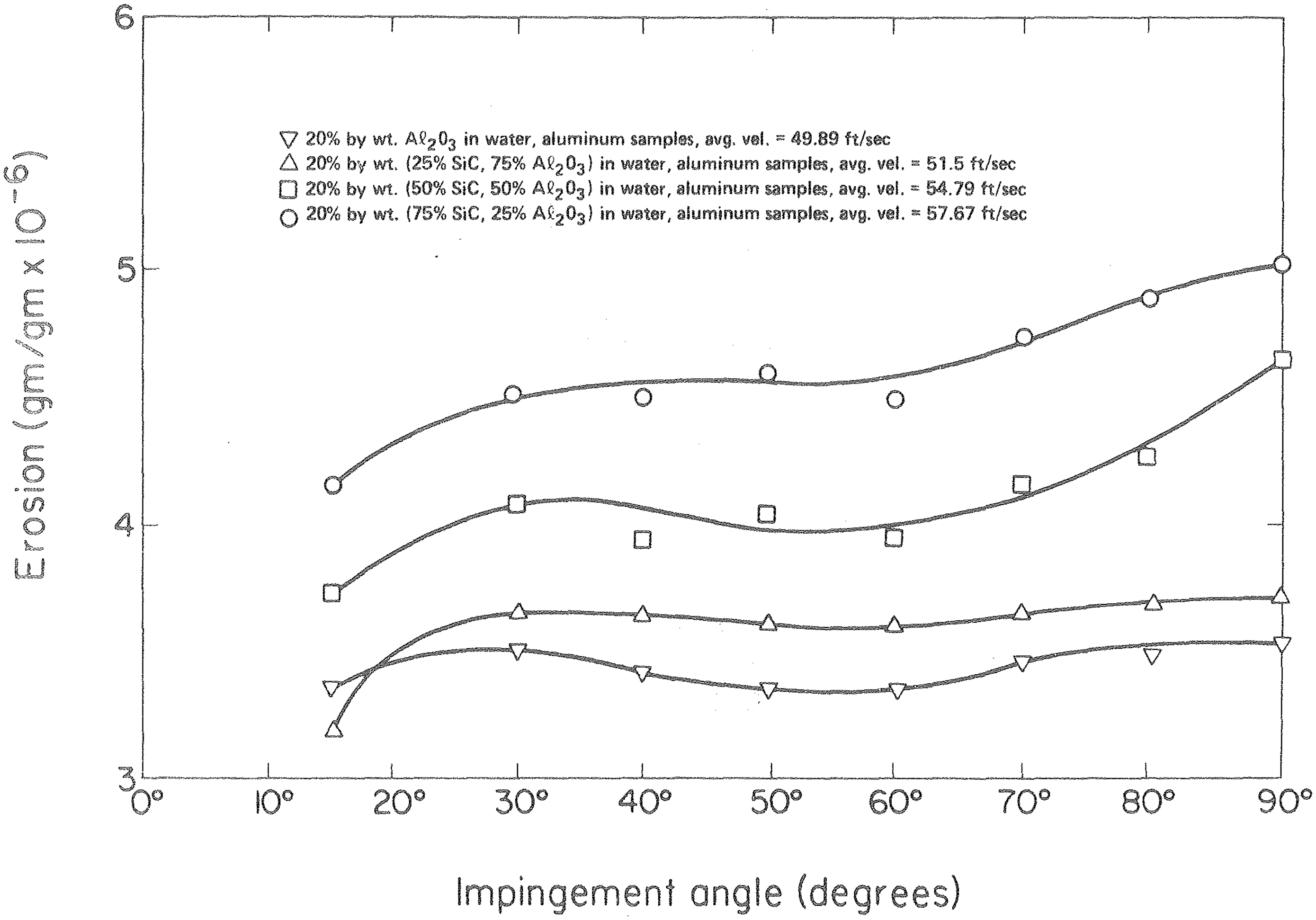

Fig. 8

XBL 8012-2457

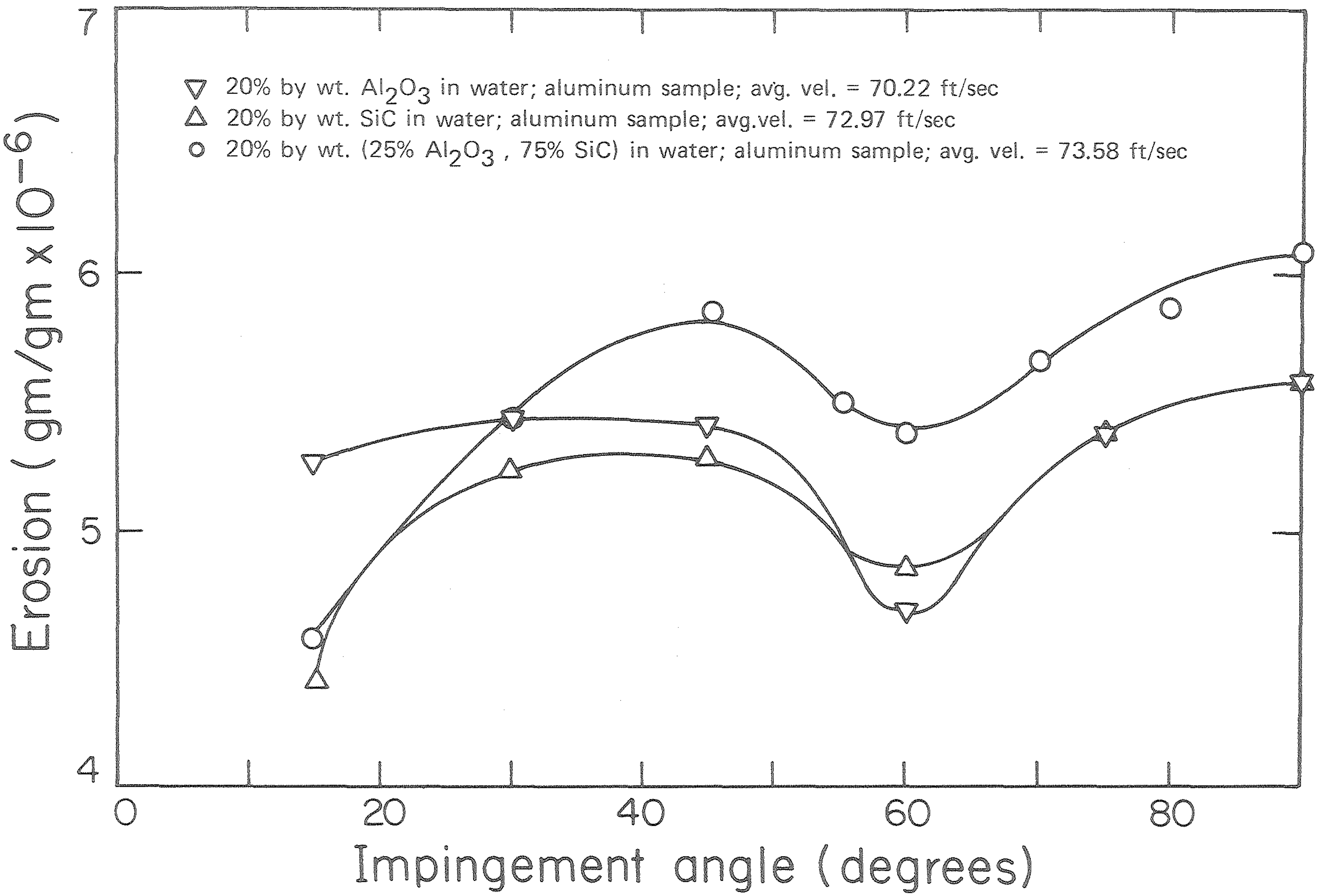

Fig. 9

XBL816-931

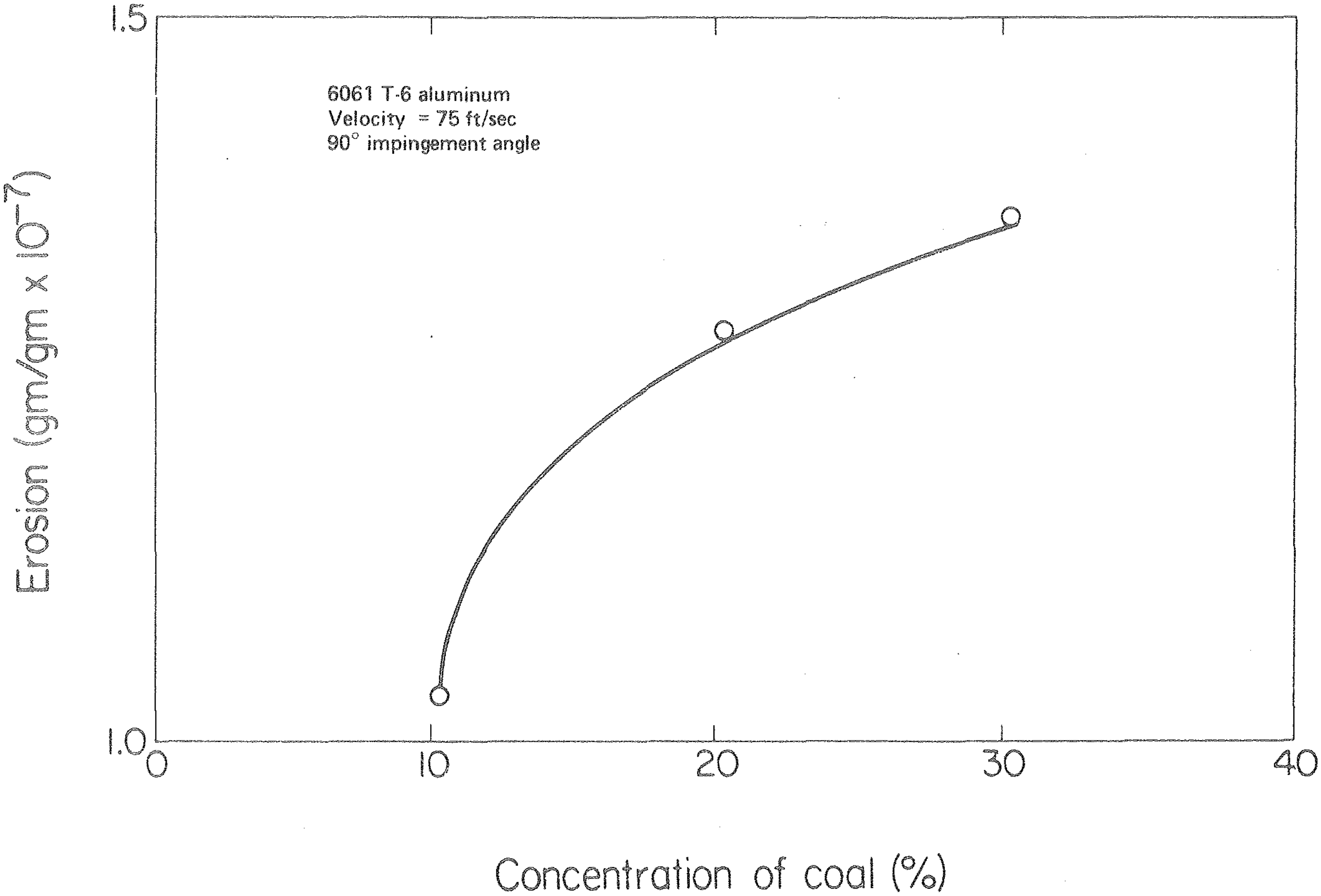

Fig. 10

XBL 8012-2452

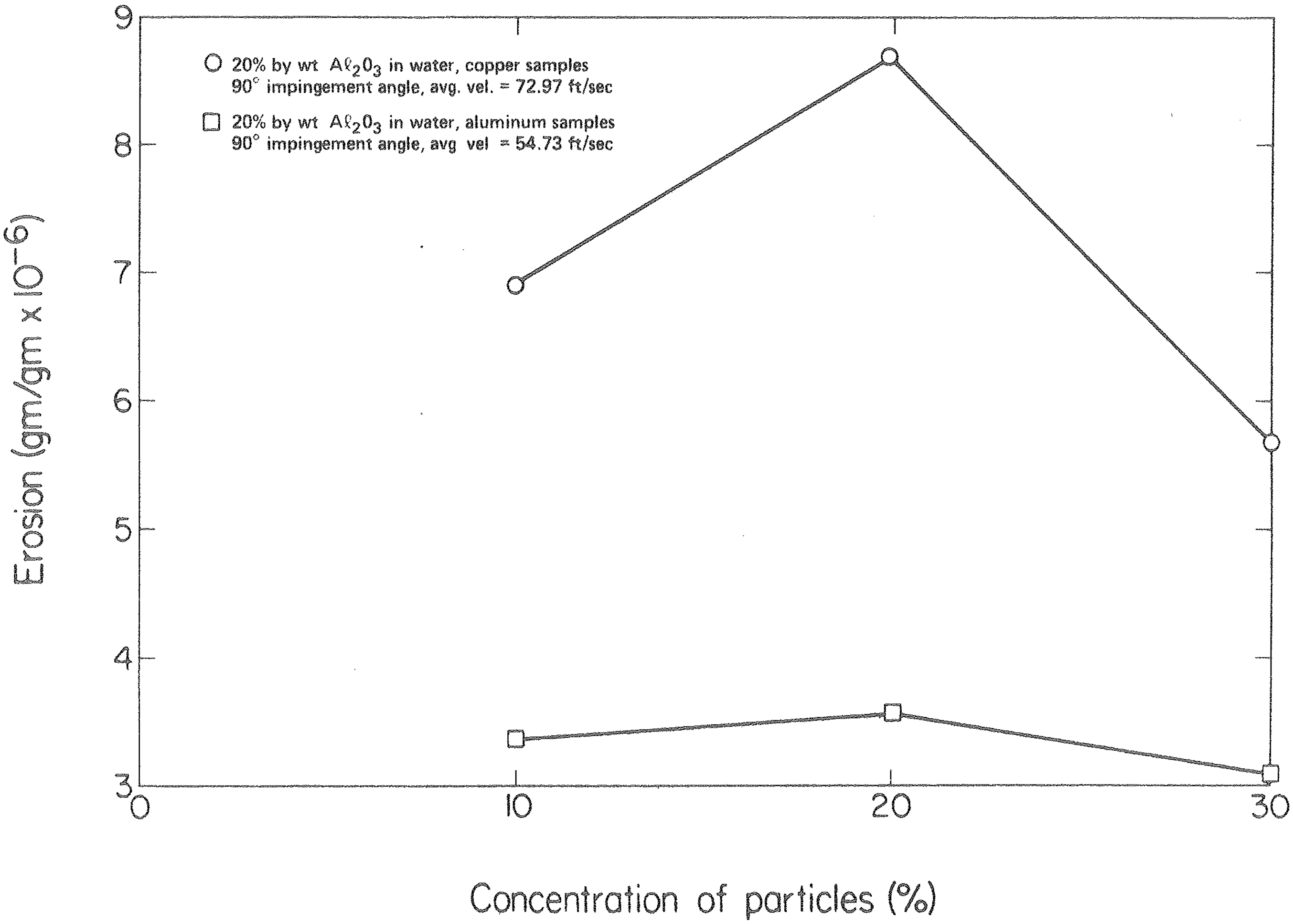

Fig. 11

XBL 8012-2455

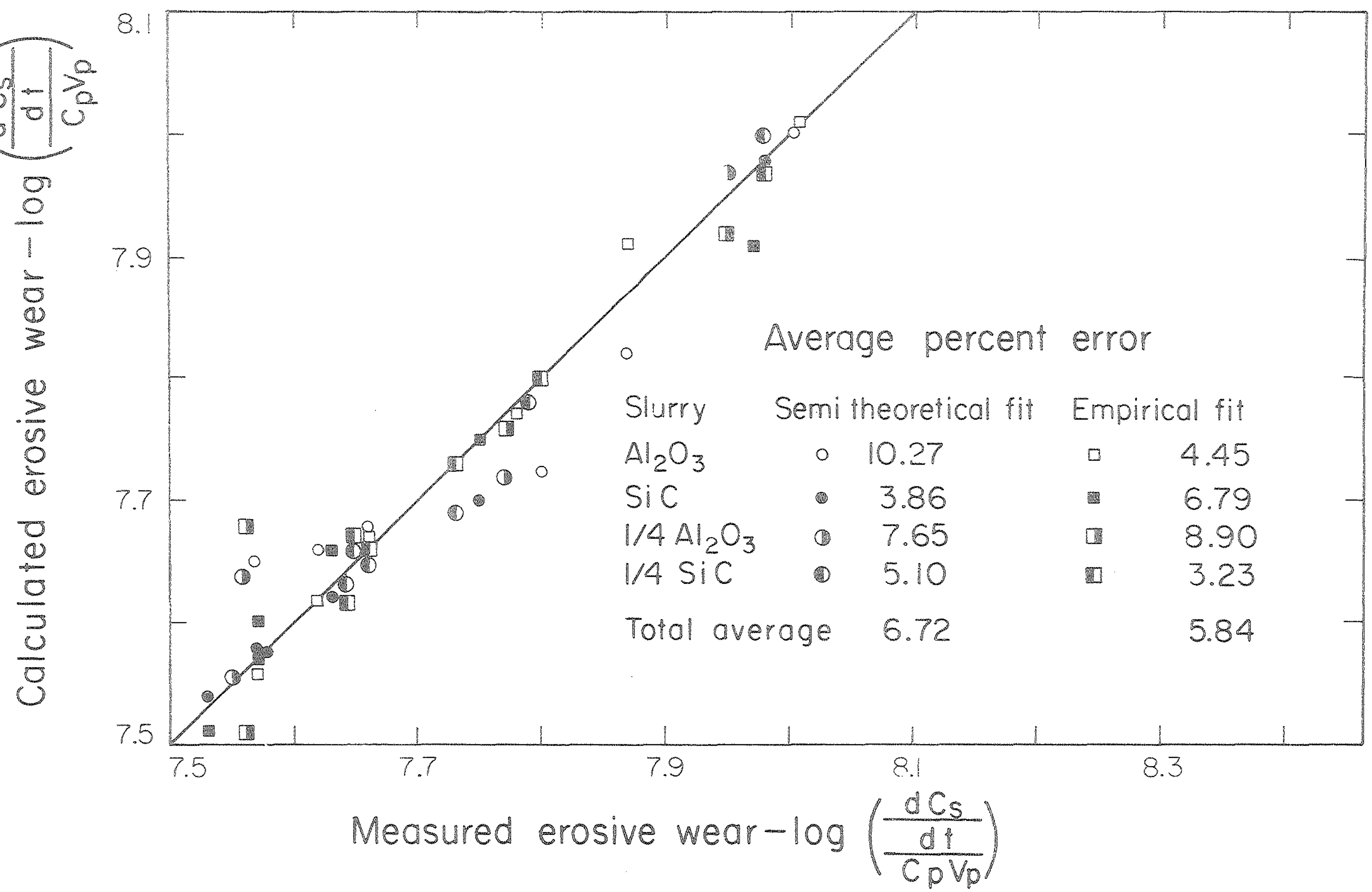

Fig. 12

XBL816-934